Thermal activation and structural succession of coal gangue in southern Sichuan, China

Jianmin Zhou (245960737@qq.com)
Chengdu Textile College
Yingru Hu
Xi'an Technological University
Dexue Chen
Chengdu Textile College
Xueli Bai
Chengdu Textile College
Yuting Ma
Chengdu Textile College
Yongsheng Fu
Southwest Jiaotong University

Research Article

Keywords: adsorption, coal gangue, thermal activation, pore size distribution, structural change

Posted Date: October 26th, 2022

DOI: https://doi.org/10.21203/rs.3.rs-2187036/v1

Abstract

Coal gangue is rich in kaolin clay minerals, which can be used as raw materials for the preparation of adsorbents and intermediates of adsorbents, and is important for the high added value utilization of coal gangue. In this study, coal gangue from southern Sichuan, China, was activated and characterized by calcination at 100~900 °C, and the succession laws of the phase, microstructure and physical properties under thermal activation conditions were studied. Results showed that the content of active hydroxyl groups in the thermally activated coal gangue was the highest, and the chemical reaction activity was highest at 800 °C for 2 h. The pore structure of thermally activated coal gangue is primarily mesoporous, which nearly disappears at 900 ℃. The specific surface area of thermally activated coal gangue is highest at 600 ℃ and lowest at 900 ℃. The results of this study provide a reference for the preparation of adsorbents and adsorbent intermediates from coal gangue.

1 Introduction

Coal gangue is a solid waste produced during raw coal extraction and washing; makes up approximately 10-20% of coal production; and is a mixed mineral composed of various minerals, water and a small amount of organic matter (Zhang and Ling, 2020). In China, the stock and production of coal gangue are large, with the accumulated stock of coal gangue reaching 7 billion t as of 2017 (Yang, 2017) , and the production continues to grow by more than 300 million t per year (Li, 2014), Cheng et al., 2018). Currently, the comprehensive utilization rate of coal gangue is less than 30% (Xie et al., 2021). The perennial stockpiled coal gangue takes up a lot of valuable land resources; damages the environment around the mining area; affects the underground water quality of the mining area; and damages the landscape (Wang et al., 2021).

Coal gangue is both a pollutant and a resource. The primary chemical composition of coal gangue includes Al_2O_3, SiO_2, Fe_2O_3, Na_2O, K_2O, CaO, MgO and other oxides (Zhou et al., 2021b). The primary mineral components are kaolinite, montmorillonite, illite, chlorite, calcite, burmite, etc., where kaolinite and montmorillonite are the primary clay minerals of coal gangue (Zhou et al., 2021b), Zhang et al., 2009). Currently, the comprehensive utilization of coal gangue primarily includes insulation materials (Zhu et al., 2015), land reclamation materials (Tang et al., 2018), ceramic products(Li et al., 2016b), filling materials (Yao and Sun, 2012) and concrete materials (Kuz'min et al., 2018). These low value-added applications are certainly a waste of the mineral resources in coal gangue. In recent years, based on the beneficial composition and mineral structure considerations of coal gangue, some scholars at home and abroad have begun to explore the comprehensive utilization of high value-added coal gangue in the field of chemical raw materials (Cheng et al., 2012), coagulants and adsorbent materials (Chen and Lu, 2018). Because coal gangue is rich in beneficial components such as aluminum, iron, titanium and silicon, it can be used to prepare polyaluminum chloride (Wang and Xin, 2012), polyaluminum ferric chloride (Kong et al., 2022), polyaluminum ferric sulfate (Chen et al., 2020) and polymeric silicate coagulants (Yang et al., 2019). Based on its beneficial mineral composition, zeolite, an adsorbent for phosphorus removal (Zhou et al., 2021a) and an adsorbent for heavy metals (Ahmadi et al., 2022) can be prepared.

Due to its low activity, small specific surface area and low porosity, raw coal gangue cannot be directly used to prepare coagulants and adsorbents; thus, it must be activated, typically via calcination. Calcination can transform well-crystallized kaolinite into reactive disordered metakaolinite and improve its surface properties (Sun et al., 2019). Currently, the preparation of coagulants and adsorbents using coal gangue is primarily performed by calcination activation to prepare active intermediates. However, most of these studies focused on the preparation process and properties, while the evolution of structure and surface properties during calcination has rarely been reported. The surface properties and pore structure of adsorbents are known to be key factors that affect the adsorption performance (Ighalo et al., 2021), Horikawa et al., 2022), Danish et al., 2022).

In this study, the chemical composition, mineral composition and surface properties of gangue in southern Sichuan were analyzed, and the succession rules of the phase, structure and physical properties of thermally activated coal gangue under different conditions were explored. The optimum roasting conditions for the preparation of adsorbents and intermediates from coal gangue were determined. Also, the thermal activation mechanism, physical phase, structure and physical properties of the gangue were systematically analyzed by X-ray diffraction (XRD), Fourier transform infrared (FTIR), scanning electron microscopy (SEM), specific surface analysis (BET), thermogravimetric-differential scanning calorimetric analysis (TGA-DSC) and other methods.

2 Materials And Methods

2.1 Material

The coal gangue used in this study was collected from Sichuan GuXu Coal Field Development Co., Ltd. (China). The raw coal gangue was manually separated to remove impurities and white gangue, and was then milled to 160 mesh with a ball mill.

2.2 Thermal activation method

A total of 20 g of 160-mesh gangue was placed in a corundum crucible and calcined at different temperatures. The coal gangue calcined at high temperature for a certain time was then removed from the muffle furnace and cooled to room temperature. After cooling, the phase, morphology, specific surface area, pore size distribution and adsorption capacity of the sample were analyzed. A thermal activation test with different holding times was performed under the best working conditions of calcination temperature, and the phase and surface functional groups of the test samples were analyzed to determine the best holding time.

2.3 Material characterization

In this study, the heat loss and heat flow change of raw coal gangue were analyzed by a TAQ600 thermogravimetric analyzer (USA), and a JEOL JEM2100 X transmission electron microscope (JEOL, Japan) was used to analyze the surface modification kinetics and morphological characteristics of the

adsorbent. A Smartlab 9kw X-ray diffractometer (RIKEN, Japan) was used to analyze the XRD and phase changes of thermally activated coal gangue with Cu K-ray radiation under the following conditions: Ni filtering at 40 KV and 40 mA; a scanning speed of 0.05 s/step; and a scanning range of 5~80°(2). A SU8100 scanning electron microscope and S4800 scanning electron microscope (Hitachi, Japan) were used to analyze the morphological characteristics of the samples at 1~120 K magnification. A PANalytical Epsilon 3XLE energy dispersive X-ray fluorescence spectrometer (PANALYTICAL, Netherlands) was used to analyze the chemical composition and content in the modified materials. A Thermo Fisher IS50 FTIR spectrometer (THERMOFISHER, USA) was used to determine the FTIR of the samples and to analyze the functional groups and chemical bonds on the surface of the samples. A JW-BK100 specific surface area analyzer (Beijing Jingwei Gaobo Science and Technology Co., Ltd) was used to analyze the specific surface area, pore size, pore size distribution, pore capacity and pore structure of the raw coal gangue and heat-activated materials.

3 Results And Discussion

3.1 Characterization of raw coal gangue

The coal gangue used in the experiment was analyzed via X-ray fluorescence, and these results are shown in Table 1. The primary components of coal gangue are SiO_2, Al_2O_3, Fe_2O_3 and TiO_2. XRD results show that (Fig. 1) the primary mineral phases of coal gangue selected in the test are quartz, kaolin, calcite and kaolinite-montmorillonite layers, of which the kaolin and kaolinite-montmorillonite layers have rich layered structures.

Table 1

Chemical composition of coal gangue (%)

Project	SiO_2	Al_2O_3	Fe_2O_3	CaO	TiO_2	MgO
Relative quantity	43.97	18.43	14.75	12.11	4.45	2.18

3.2 Structural succession of thermally activated coal gangue

3.2.1 TGA-DSC analysis

The TGA-DCS curve of gangue is shown in Fig. 2. There are three troughs at 108.04℃, 503.92℃ and 748.7℃ and two peaks at 453.00℃ and 676.44℃. The trough at 108.04 °C is primarily caused by the desorption of water adsorbed on the surface of gangue. The trough at 503.92 °C is caused by the endothermic conversion of kaolinite into metakaolinite due to the loss of crystalline water. The trough at 748.7 °C is caused by the heat absorption of calcite decomposition. The wave peak at 453.00 °C may be the exothermic peak generated by the combustion of organic matter in gangue, while the wave peak at 676.44 °C may be caused by the combustion of carbon in gangue. The DSC curves from 0 to 1200 ℃ show that the gangue warming process experienced 3 phase changes. The TGA curve shows

that the process of gangue warming experienced 4 stages of weight loss. The first stage is the slow weight loss stage at 50~200 °C. The weight loss in this stage is primarily caused by the desorption of adsorbed water from coal gangue, and the weight loss rate was 1.775%. The second stage is primarily the stage of accelerated weight loss at 200~600 °C. The weight loss in this stage is primarily caused by the conversion of organic matter in the gangue into carbon dioxide and water, and the loss of crystalline water in kaolin, with a weight loss rate of 4.986% (Hao et al., 2022). The third stage is the rapid weight loss stage at 600~800 °C. The weight loss in this stage is primarily caused by the decomposition of calcite to overflow carbon dioxide and the combustion of carbon to form carbon dioxide overflow, and the weight loss rate is 5.943% (Li et al., 2016a). The fourth stage is the stable weight loss stage at 800~1200℃. The weight loss in this stage is primarily caused by the desiccation of internal structure water. Thus, the temperature of gangue thermal activation should be selected after the decomposition of kaolin and calcite but before the formation of a new stable mineral phase (i.e., above 748.7 °C).

3.2.2 Succession law of ore facies of thermally activated coal gangue

The X-ray diffraction patterns of raw coal gangue and coal gangue calcined at 200~900 °C are shown in Fig. 3a. With calcination at 200~500 °C, the mineral phases of quartz and calcite remained unchanged, while the peaks of kaolinite-montmorillonite and kaolin gradually decreased with increasing calcination temperature. The peaks of kaolinite and kaolinite-montmorillonite were not found in the coal gangue calcined at 600 °C, indicating that the kaolin has been completely transformed into metakaolin at 600 °C. The calcite characteristic peak began to weaken at 700 °C, which is consistent with the results of differential thermal analysis. The characteristic peaks of calcite disappeared at 800 °C; thus, the reaction activity of thermally activated coal gangue was the strongest at 800 °C. To describe the effect of holding time on the phase structure of coal gangue, the coal gangue was calcined at 800 ℃ for 0.5, 1.0, 2.0, 3.0 and 5 h of holding time. After natural cooling, the XRD patterns of the calcined samples under different holding times were analyzed (Fig. 3b). Results show that the XRD pattern waveforms of thermally activated coal gangue with different holding times are similar.

3.3 Succession law of the physical properties of thermally activated coal gangue

3.3.1 FTIR analysis of thermally activated coal gangue

The FTIR spectrum of coal gangue shown in Fig. 4a indicates that the absorption peak at 3696 cm^{-1} is formed by the vibration of the outer kaolinite hydroxyl (Al-O-H, structural water) in the coal gangue; the absorption peak at 3623 cm^{-1} is formed by the vibration of hydroxyl groups (interlayer water between silicon oxygen tetrahedron and aluminum oxygen octahedron) in kaolin(Torres-Luna and Carriazo, 2019), Madejová, 2003); the absorption peak at 796 cm^{-1} is formed by the vibration of Si-O-Si in kaolin; and the absorption peak at 694 cm^{-1} is formed by the strong bending vibration of Si-O in kaolin (Li et al., 2019). These results are consistent with the result of kaolin contained in coal gangue analyzed by XRD in Fig. 3. The absorption peak at 3431 cm^{-1} should be formed by the telescopic vibration of adsorbed water in coal gangue. The absorption peak at 1426 cm^{-1} can be attributed to the absorption frequency of Ca in calcite,

which is formed by the reverse asymmetric stretching vibration of the vertical C-axis of the CO_3^{2-}group. The absorption peak at 877.26 cm^{-1} can be attributed to the reverse bending vibration of the CO_3^{2-}group of calcite parallel to the C axis (Sruthi and Reddy P, 2017), Ferone et al., 2015), which indicates that the coal gangue contains calcite. There is also a weak absorption peak at 1088 cm^{-1}, which is formed by the stretching vibration of the Si-O bond in montmorillonite and should be formed by the expansion and contraction vibration of the Si-O bond in the high mask mixed layer in the coal gangue. The absorption peak at 1031 cm^{-1} should be formed by the asymmetric stretching vibration of the Si(Al)-O-Si bond (Li et al., 2015). The infrared spectrum shows few changes below 500 ℃. The absorption peaks near 3696, 3623 and 694 cm^{-1} began to weaken at 500 °C. At 600 °C, the absorption peaks near 3696 cm^{-1} and 3623 cm^{-1} disappeared, while the absorption peak at 694 cm^{-1} shifted to 690 cm^{-1} and nearly disappeared, indicating that at 600 °C, the kaolinite in the coal gangue was almost completely converted to metakaolinite. The absorption peak at 1426 cm^{-1} moved in the direction of the wavenumber decrease with increasing temperature and started to weaken at 700 ℃. The absorption peak at 877.26 cm^{-1} moved in the direction of increasing wavenumber with increasing temperature and began to weaken at 700 °C. The absorption peaks near 1426 cm^{-1} and 877 cm^{-1} disappeared at 800 ℃, indicating that calcite completely decomposed at 800 ℃. At 700℃, a faint absorption peak appears at 3642 cm^{-1}, which may be formed by hydroxyl stretching vibrations of Al-OH and Ca-OH (, 2010), where the absorption peak is enhanced at 800℃ and the absorption peak is weakened at 900℃, indicating that a new substance may form at 700℃, and this new material is most abundant at 800℃. At 900 ℃, in addition to the adsorption of water, only the absorption peak of quartz is left, and the adsorption of water in this study may be formed by incomplete drying of the material. The absorption peak at 1031 cm^{-1} gradually moved toward the direction of increasing wavenumber with increasing temperature, and widening occurred, which indicates that the spacing between layered silica tetrahedron structures is reduced due to the release of interlayer structural water from clay minerals during calcination. Also, widening begins after 600 ℃ because the crystallinity of silica tetrahedron decreases with increasing temperature (Zhang, 2010). The characteristic peak of quartz at 796 cm^{-1} is weak below 400 °C, and the characteristic peak begins to strengthen at 400~600 °C, which is due to the increase in the relative concentration of quartz caused by the combustion of carbon in gangue and the removal of hydroxyl groups in kaolin. The FTIR spectrum waveform of thermally activated gangue with different holding times were similar, and the absorption peak near 3642 cm^{-1} first increased and then decreased with increasing holding time. The peak was the highest at 2 h (Fig. 4b), which showed that the activity of thermally activated gangue was the strongest at 2 h.

3.3.2 Effect of activation temperature on the morphological characteristics of coal gangue

Fig. 5a shows an SEM image of the unburned coal gangue. The surface structure of the unburned coal gangue is relatively compact, and the structure of the thermally activated coal gangue at 200~500 ℃ is similar (Fig. 5b, c, d, e), maintaining the original structural state of the coal gangue. At 600 ℃, the layered structure of thermally activated coal gangue loosens, which may occur because the hydroxyl group of

kaolin is removed to reduce the binding of the layered structure, which makes the interlayer structure loose. The relaxation of the crystal structure is conducive to improving the porosity of coal gangue (Fig. 5f). The layered structure of activated gangue at 700~800℃ did not change markedly, but the relaxation of the crystal structure increased due to the loss of interlayer water (Fig. 5g, h). The layered structure of activated coal gangue at 900 ℃ markedly changed: the layered structure collapses, which makes the porosity and surface area drop markedly (Fig. 5i, j).

3.3.3 Absorption and desorption curve of thermally activated coal gangue

The pore structure of the thermally activated coal gangue sample at different temperatures was characterized by an adsorption-desorption isotherm of N_2 at 77 K, and the results are shown in Fig. 6. The N2 suction-desorption isotherm of the coal gangue sample with a thermal activation temperature of less than 800℃ is similar. According to the classification basis proposed by the International Union of Pure and Applied Chemistry (IUPAC), the heat activation temperature of less than 800℃ of the coal gangue suction and desorption isotherm is in line with the characteristics of the V-type isothermal and H3 hysteresis loop. These results show that the structure of the pores in the gangue soil, and that the sample heated to 800℃ is primarily mesoporous, which can be attributed to the slit hole formed by the accumulation of layered particles (Thommes et al., 2015). At low relative pressure (p/p_0 0.4), the adsorption amount of N_2 slowly increases with increasing relative pressure, at which time the adsorption branch line and the desorption branch line completely coincide, primarily mesoporous monolayer adsorption, and no microporous adsorption is present (Kresge et al., 1992). As the relative pressure rises again, the adsorption of N_2 increases markedly and forms a hysteresis loop with the desorption branch, which is primarily due to the phenomenon of capillary condensation of the mesoporous material during nitrogen suction and desorption. Adsorption is caused by two factors: multilayered adsorption of pore walls and agglomeration in the pores, while desorption is only caused by capillary agglomeration. Thus, multimolecular layer adsorption first occurs during adsorption, and condensation can only occur when the adsorption layer on the pore wall reaches a sufficient thickness. When desorption occurs under the pressure of the same p/p_0 ratio, the steam that occurs only on the liquid surface in the capillary cannot desorb the molecules adsorbed under p/p_0, and to desorb, a smaller p/p_0 is required; thus, the lag phenomenon of desorption occurs, which is actually caused by the irreversibility of adsorption under the same p/p_0. The shape of the hysteresis loop reflects a certain pore structure, reflecting a slit mesoporous produced by a flaky granular material in the pores of thermally activated coal gangue below 800 ℃(Jin et al., 2021), Thommes et al., 2015).

According to the Kelvin equation and capillary coagulation theory, the early and late closure of the upper and lower ends of the hysteresis loop indicates the width and narrowness of the mesoporous pore size distribution, respectively; the farther the upper and lower ends of the closure point are, the wider the mesoporous aperture distribution. Also, the closer the upper and lower end closure points are, the narrower the pore size distribution of the mesopore. Fig.6 shows that the gangue and activation products below 800℃ are primarily mesoporous, and the distribution of mesoporous pore size does not change

much. The absorption and desorption isotherm of the thermally activated gangue product at 900℃ is nearly straight, the adsorption amount is small, and the hysteresis loop is also almost gone, indicating that the pores in the activated gangue samples gradually disappear at this temperature.

3.3.4 Succession law of the specific surface area of thermally activated coal gangue

The multipoint BET method was used to analyze the succession law of the specific surface area of thermally activated coal gangue. The specific surface area of coal gangue first decreases, then increases, and finally decreases with increasing calcination temperature (Fig. 7a). Calcined coal gangue at 200℃ shows a large decrease in the specific surface area of the original soil due to the decrease in the specific surface area caused by the shrinkage of the clay minerals in the coal gangue, which is caused by the shrinkage of the crystals due to the adsorption of water. The specific surface area of coal gangue calcined at 200~300 ℃ continues to decrease, which is primarily due to the continuous stripping of interlayer water of layered silicate minerals with increasing temperature, which causes interlayer hydrogen bond fracture, resulting in the reduction of part of the interlayer spacing and the reduction of the specific surface area caused by overlap. The specific surface area of coal gangue calcined at 300~600 ℃ increases slowly with increasing temperature, which is primarily caused by two aspects. First, the increase in mesopores caused by the combustion of coal gangue carbon increases the specific surface area. The other is that the specific surface area increases due to the increase in mesopores and micropores caused by the dehydration of layered silicate mineral structure water. The specific surface area of coal gangue calcined at 600~800 ℃ decreases with increasing temperature, which is due to the layered structure sintering of silicate minerals caused by the increase in temperature and the pore blockage caused by the decomposition of calcite caused by the increase in temperature. The specific surface area of calcined coal gangue at 900 ℃ dropped to below 4.00 m^2/g, indicating that the layered structure began to collapse at 900 ℃.

3.3.5 Pore size and pore volume succession of thermally activated coal gangue

The size, shape and number of pores have a great influence on the measurement results of the surface area. Concurrently, the pore volume and pore diameter of materials strongly affect the adsorption, catalysis, stability, subsequent modification and loading of the materials themselves. The change in average aperture shows a rising-decreasing-rising-decreasing-rising trend (Fig. 8a). The increase in the pore diameter of coal gangue calcined at 200 ℃ may be due to the removal of adsorbed water and the shrinkage of its structure. The decrease in the pore diameter of coal gangue calcined at 300 ℃ may be caused by the desorption of interlayer water. The increase in the calcined coal gangue pore diameter at 300~500 ℃ may be caused by the combustion of carbon in coal gangue. The decrease in the average pore diameter of coal gangue calcined at 500~600 ℃ is primarily caused by the increase in micropores due to the loss of kaolin crystal water. The increase in the average pore diameter of coal gangue calcined at 600~800 ℃ is primarily caused by the increase in mesopores caused by the deformation of Si-O bonds and Al-O bonds. The change rule of pore volume is the same as that of

specific surface area (Fig. 8b), showing a trend of first decreasing, then increasing, and then decreasing. The specific reasons are basically the same as those that cause the change in specific surface area.

3.3.6 Pore size distribution of thermally activated coal gangue

The pore size distribution of porous materials affects the adsorption, permeation, filtration and loadability of the material. In this study, the pore size of coal gangue and its thermal activated products is primarily mesoporous, and micropores can be ignored. Therefore, the BJH (Barrett Joyner Halenda) model is used to analyze the pore size distribution of coal gangue and its thermally activated products. When using the BJH method to analyze the pore size distribution, it is also necessary to consider the use of adsorption branch or desorption branch data. The desorption process generally considered to be more similar to the physical process; thus, many scholars choose to use desorption branch data to analyze the pore size distribution of mesoporous materials. Determination of pore size distribution and porosity of solid materials by mercury intrusion method and gas adsorption method - Part 2: Analysis of mesopores and macropores by gas adsorption method (GBT21650.2-2008) provides suggestions about the selection of mesoporous analysis data and notes that careful analysis should be performed. For the narrow H1 hysteresis curve produced by the relatively simple hole structure of a relatively uniform cylindrical hole, the desorption branch of the curve is often used for aperture analysis. When the connecting hole is plugged, producing seepage, it is unsafe to use the adsorption branch or desorption branch because there may be a mixing effect with both delayed agglutination and network penetration. If a certain method is used to consider the influence of pore size on delayed agglutination, particularly in the metastable range of pore fluid, the adsorption branch can be used for pore size analysis. If the so-called "tension strength effect" occurs during evaporation, the desorption branch of the curve will drop markedly at a certain P/P0, which varies with the type and temperature of the adsorbed gas. For the adsorbed gas of 77 K N2, the p/p0 value is 0.42. A more realistic pore size distribution can be obtained according to the adsorption branch of the curve. The H3 hysteresis ring appears in the N_2 adsorption and desorption curve of coal gangue and thermal activation products (Fig. 6), which indicates that the pores in the material are irregular, and the so-called "tensile strength effect" occurs during evaporation; thus, the pore size distribution curve of coal gangue and heat-activated coal gangue in this paper is calculated by adsorption branches. The radius corresponding to the highest peak in the differential curve is the most likely pore size.

As shown in Fig. 9, the pore size distribution curve of the BJH adsorption branch of raw coal gangue and thermally activated coal gangue at different temperatures shows that there is only one peak of raw coal gangue and thermally activated products, which indicates that the pore size distribution is relatively concentrated. The position and intensity of the peak fluctuate with increasing thermal activation temperature (Table 2). The peak position of calcined coal gangue (including 300 ℃ calcined coal gangue) remains consistent below 300 ℃, which indicates that the pore structure of thermally activated coal gangue undergoes few changes within this temperature range. The peak position of coal gangue calcined at 400 ℃ was pushed back to 2.8192 nm, which may be caused by the combustion of C in coal gangue. The peak position of coal gangue calcined at 500 ℃ returns to 2.4903 nm, the peak position of

coal gangue calcined at 600~700 ℃ returns to 2.8 nm, and the peak position of coal gangue calcined at 800 ℃ or above returns to 2.5 nm, which may be caused by the decomposition of calcite. The intensity change of the peak is thus dependent on the change in pore volume, and the peak effectively disappears at 900 °C, which indicates that the structure has effectively collapsed at 900 °C.

Table 2

Most probable pore size and strength of activated coal gangue at different temperatures

Sample	Most probable pore size nm	dV/D(cc/nm/g)
raw	2.5174	0.00878
200℃	2.4784	0.00374
300℃	2.4881	0.00253
400℃	2.8192	0.00313
500℃	2.4903	0.00441
600℃	2.7867	0.00628
700℃	2.8303	0.00447
800℃	2.4629	0.00332
900℃	2.4845	0.00139

4. Conclusions

Gangue in southern Sichuan is rich in kaolin and kaolinite-montmorillonite, which can be used as an adsorbent and adsorbent intermediate after heat activation. The content of hydroxy active hydroxyl groups and the chemical reaction activity of thermally activated coal gangue are the highest at 800 ℃ for 2 h.

The pore structure of coal gangue thermally activated at 800 ℃ or below is primarily mesoporous, and no micropores are found. The mesopores of coal gangue thermally activated at 900 ℃ nearly disappear. With increasing activation temperature, the specific surface area of thermally activated coal gangue shows a trend of first decreasing, then increasing, and finally decreasing. The specific surface area of calcined coal gangue at 600 ℃ is the highest of those measured in this study (approximately 15 m^2/g), while that at 900 ℃ is the lowest (less than 4 m^2/g). The average pore diameter of BJH first increases, then decreases, and then slowly increases. The average pore diameter of calcined coal gangue is maximized at 500 ℃ and minimized at 600 ℃. The pore volume first decreases, then increases, and finally decreases with temperature, and the pore volume of coal gangue calcined at 600 ℃ is the highest. The most likely pore size does not vary much with temperature and fluctuates between 2.46 and 2.83. The most likely pore size of calcined coal gangue is the smallest at 300 ℃ and the largest at 700 ℃.

Declarations

Acknowledgments

The work was supported by Sichuan Science and Technology Program NO 2021YFG0262 .

References

1. H Ahmadi, Duan Y, Hussain S, et al. (2022) An Effective Method for Adsorption of Pb^{2+} , Cd^{2+} , and Cu^{2+} from Wastewater by Using NaXZeolite-Derived from Coal Gangue. OALib 09: 1-12.
2. J Chen, Li X, Cai W, et al. (2020) High-efficiency extraction of aluminum from low-grade kaolin via a novel low-temperature activation method for the preparation of poly-aluminum-ferric-sulfate coagulant. Journal of Cleaner Production 257: 120399.
3. J Chen, Lu X (2018) Equilibrium and kinetics studies of Cd(II) sorption on zeolite NaX synthesized from coal gangue. Journal of Water Reuse and Desalination 8: 94-101.
4. F Cheng, Cui L, Miller J D, et al. (2012) Aluminum Leaching from Calcined Coal Waste Using Hydrochloric Acid Solution. Mineral Processing and Extractive Metallurgy Review 33: 391-403.
5. Y Cheng, Hongqiang M, Hongyu C, et al. (2018) Preparation and characterization of coal gangue geopolymers. Construction and Building Materials 187: 318-326.
6. M Danish, Ansari K B, Danish M, et al. (2022) A comprehensive investigation of external mass transfer and intraparticle diffusion for batch and continuous adsorption of heavy metals using pore volume and surface diffusion model. Separation and Purification Technology 292: 120996.
7. C Ferone, Liguori B, Capasso I, et al. (2015) Thermally treated clay sediments as geopolymer source material. Applied Clay Science 107: 195-204.
8. R Hao, Li X, Xu P, et al. (2022) Thermal activation and structural transformation mechanism of kaolinitic coal gangue from Jungar coalfield, Inner Mongolia, China. Applied Clay Science 223: 106508.
9. T Horikawa, Okamoto M, Kuroki-Matsumoto A, et al. (2022) Significant role of counterion for lead( ) ion adsorption on carbon pore surface. Carbon 196: 575-588.
10. J O Ighalo, Iwuozor K O, Igwegbe C A, et al. (2021) Verification of pore size effect on aqueous-phase adsorption kinetics: A case study of methylene blue. Colloids and Surfaces A: Physicochemical and Engineering Aspects 626: 127119.
11. J Jin, Li P, Chun D H, et al. (2021) Defect dominated hierarchical Ti-metal-organic frameworks via a linker competitive coordination strategy for toluene removal. Advanced Functional Materials 31: 2102511.
12. D Kong, Zhou Z, Song S, et al. (2022) Preparation of Poly Aluminum-Ferric Chloride (PAFC) Coagulant by Extracting Aluminum and Iron Ions from High Iron Content Coal Gangue. Materials 15: 2253.

13. C Kresge, Leonowicz M, Roth W J, et al. (1992) Ordered mesoporous molecular sieves synthesized by a liquid-crystal template mechanism. nature 359: 710-712.
14. M P Kuz'min, Larionov L M, Kondratiev V V, et al. (2018) Use of the burnt rock of coal deposits slag heaps in the concrete products manufacturing. Construction and Building Materials 179: 117-124.
15. C Li, Fu L, Ouyang J, et al. (2015) Kaolinite stabilized paraffin composite phase change materials for thermal energy storage. Applied Clay Science 115: 212-220.
16. J Li (2014) discussed the impact of coal gangue accumulation in Yangquan. Mining area on surrounding soil Land and resources in North China: 96-98
17. J Li, Zuo X, Zhao X, et al. (2019) Insight into the effect of crystallographic structure on thermal conductivity of kaolinite nanoclay. Applied Clay Science 173: 12-18.
18. L Li, Zhang Y, Zhang Y, et al. (2016a) The thermal activation process of coal gangue selected from Zhungeer in China. Journal of Thermal Analysis and Calorimetry 126: 1559-1566.
19. Z Li, Luo Z, Li X, et al. (2016b) Preparation and characterization of glass–ceramic foams with waste quartz sand and coal gangue in different proportions. Journal of Porous Materials 23: 231-238.
20. J Madejová (2003) FTIR techniques in clay mineral studies. Vibrational spectroscopy 31: 1-10.
21. P L Sruthi, Reddy P H P (2017) Characterization of kaolinitic clays subjected to alkali contamination. Applied Clay Science 146: 535-547.
22. T Sun, Ge K, Wang G, et al. (2019) Comparing pozzolanic activity from thermal-activated water-washed and coal-series kaolin in Portland cement mortar. Construction and Building Materials 227: 117092.
23. Q Tang, Li L, Zhang S, et al. (2018) Characterization of heavy metals in coal gangue-reclaimed soils from a coal mining area. Journal of Geochemical Exploration 186: 1-11.
24. M Thommes, Kaneko K, Neimark A V, et al. (2015) Physisorption of gases, with special reference to the evaluation of surface area and pore size distribution (IUPAC Technical Report). Pure and applied chemistry 87: 1051-1069.
25. J Torres-Luna, Carriazo J (2019) Porous aluminosilicic solids obtained by thermal-acid modification of a commercial kaolinite-type natural clay. Solid State Sciences 88: 29-35.
26. H Wang, Fang X, Du F, et al. (2021) Three-dimensional distribution and oxidation degree analysis of coal gangue dump fire area: a case study. Science of The Total Environment 772: 145606.
27. R G Wang, Xin Y L 2012. Preparation and wastewater treatment of polymeric aluminum chloride from coal gangue [C] //, Trans Tech Publ; City. 780-783.
28. M Xie, Liu F, Zhao H, et al. (2021) Mineral phase transformation in coal gangue by high temperature calcination and high-efficiency separation of alumina and silica minerals. Journal of Materials Research and Technology 14: 2281-2288.
29. L Y ang (2017) Talked about the comprehensive utilization of coal gangue. Sinopec: 54-55
30. Y Yang, Zeng F, Zhao Q, et al. 2019. Study on the flocculation condition of Poly-Silicate-Aluminum-Ferric (PSiAF) coagulant prepared with coal gangue as raw material [C] //, IOP Publishing; City.

042018.
31. Y Yao, Sun H (2012) A novel silica alumina-based backfill material composed of coal refuse and fly ash. J Hazard Mater 213-214: 71-82.
32. J Zhang (2010) Research on the influence of activated coal gangue and its mortar concrete on the corrosion behavior of reinforcement . Tsinghua University.
33. N Zhang, Sun H, Liu X, et al. (2009) Early-age characteristics of red mud–coal gangue cementitious material. Journal of Hazardous Materials 167: 927-932.
34. Y Zhang, Ling T-C (2020) Reactivity activation of waste coal gangue and its impact on the properties of cement-based materials–a review. Construction and Building Materials 234: 117424.
35. J Zhou, Fu Y, Pan S (2021a) The use of modified coal gangue for the remediation and removal of phosphorus in an enclosed water area. Clean Technologies and Environmental Policy 23: 1327-1339.
36. J Zhou, Fu Y, Zhang M, et al. (2021b) Removal of phosphate from water using lanthanum-modified coal gangue. DESALINATION AND WATER TREATMENT 211: 229-240.
37. P Zhu, Zheng M, Zhao S, et al. (2015) Synthesis and thermal insulation performance of silica aerogel from recycled coal gangue by means of ambient pressure drying. Journal of Wuhan University of Technology-Mater. Sci. Ed. 30: 908-913.

Figures

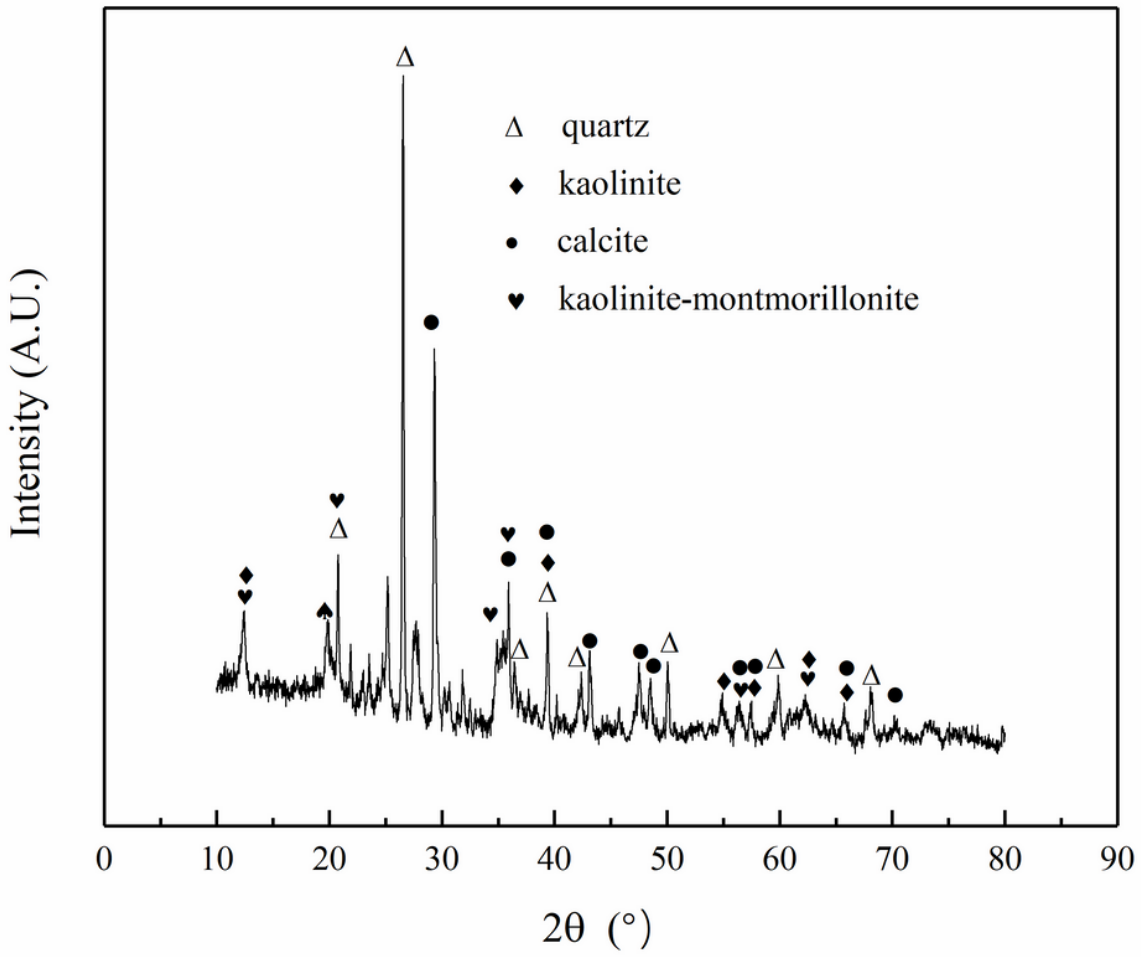

Figure 1

XRD patterns of raw coal gangue

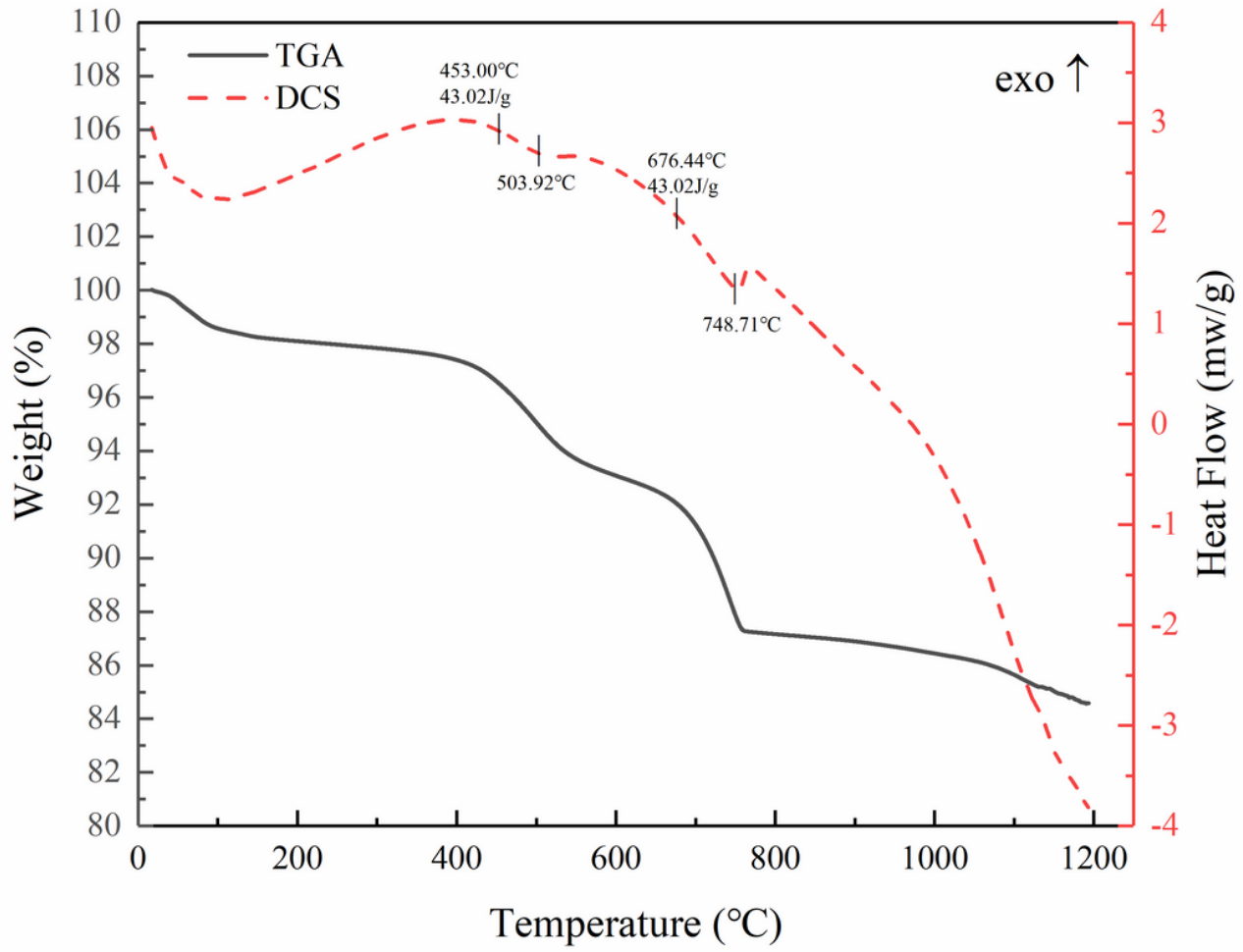

Figure 2

TG-DCS curve of coal gangue

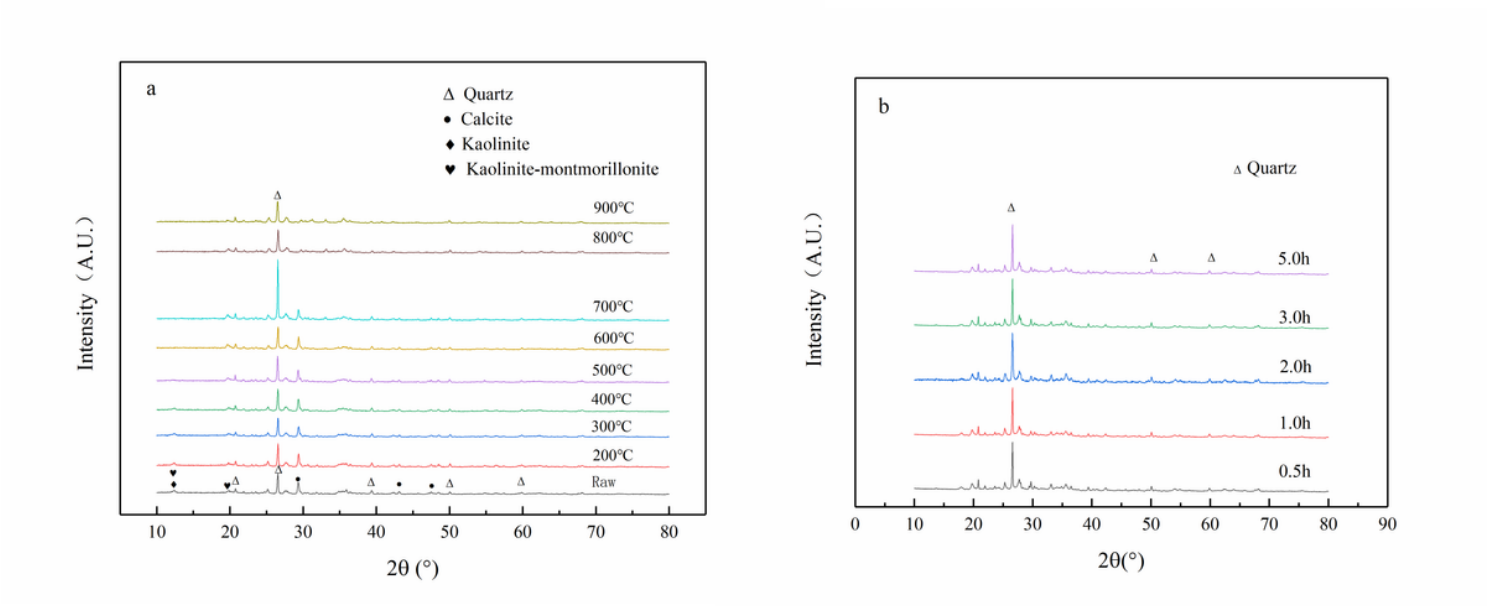

Figure 3

XRD patterns of thermally activated coal gangue at different calcination temperatures (a) and holding times (b)

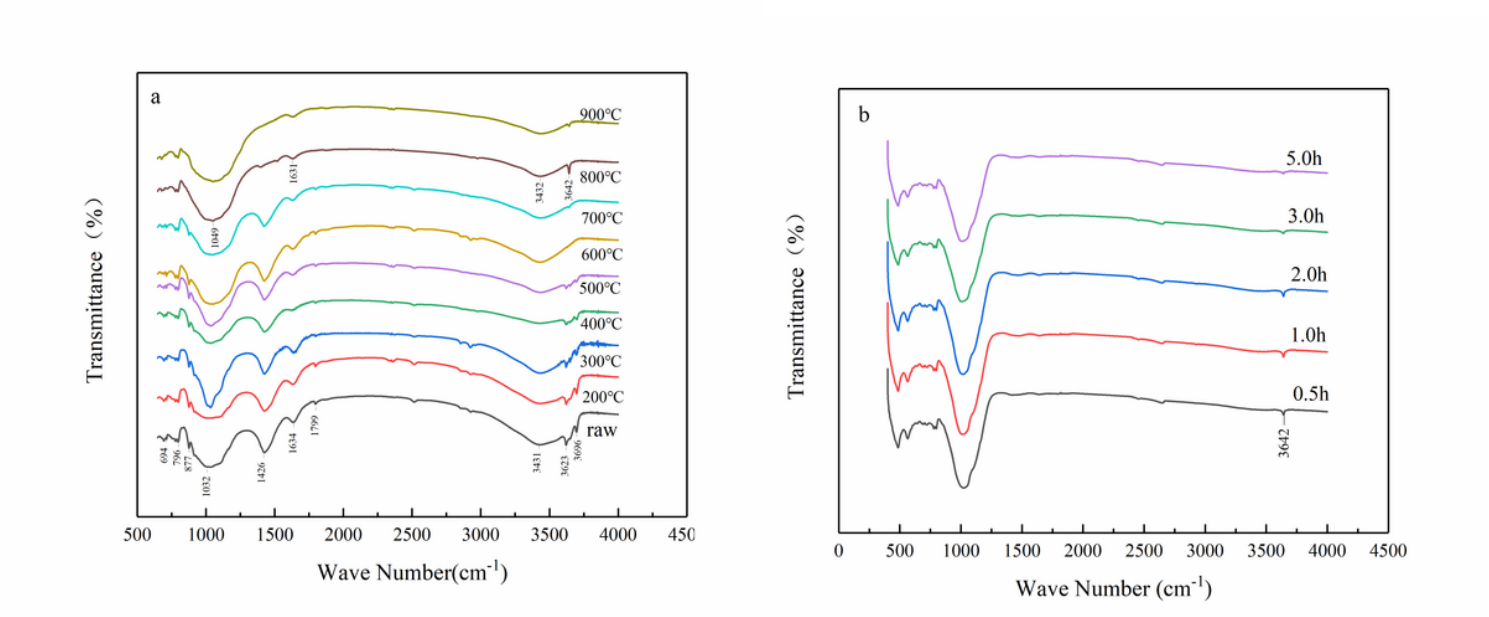

Figure 4

FTIR spectra of thermally activated coal gangue with different activation temperatures (a) and holding times (b).

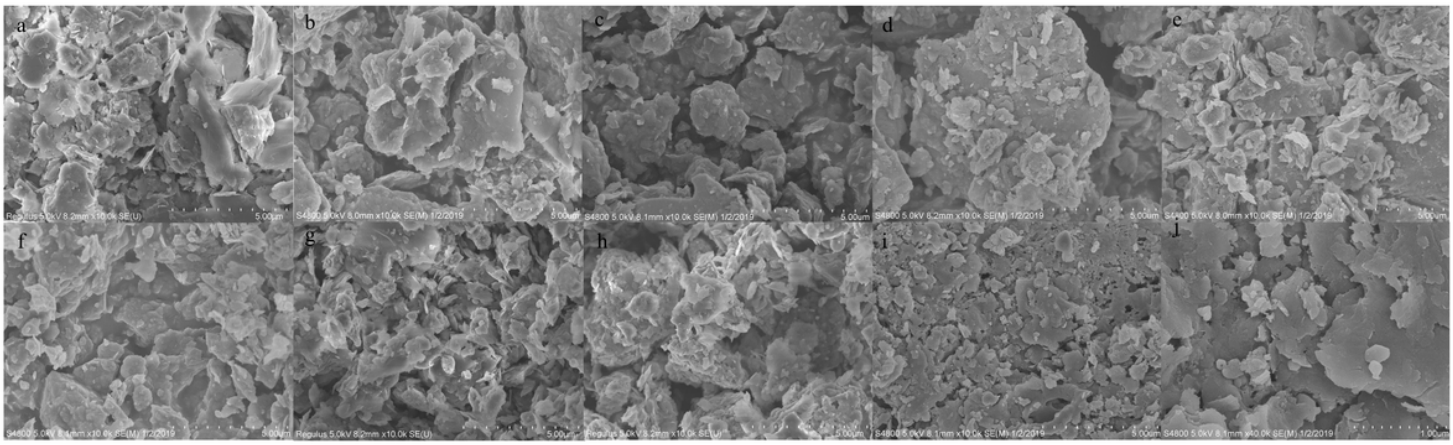

Figure 5

SEM photos of thermally activated coal gangue at different temperatures (a is untreated coal gangue, b is 200 ℃, c is 300 ℃, d is 400 ℃, e is 500 ℃, f is 600 ℃, g is 700 ℃, h is 800 ℃, i and j are 900 ℃)

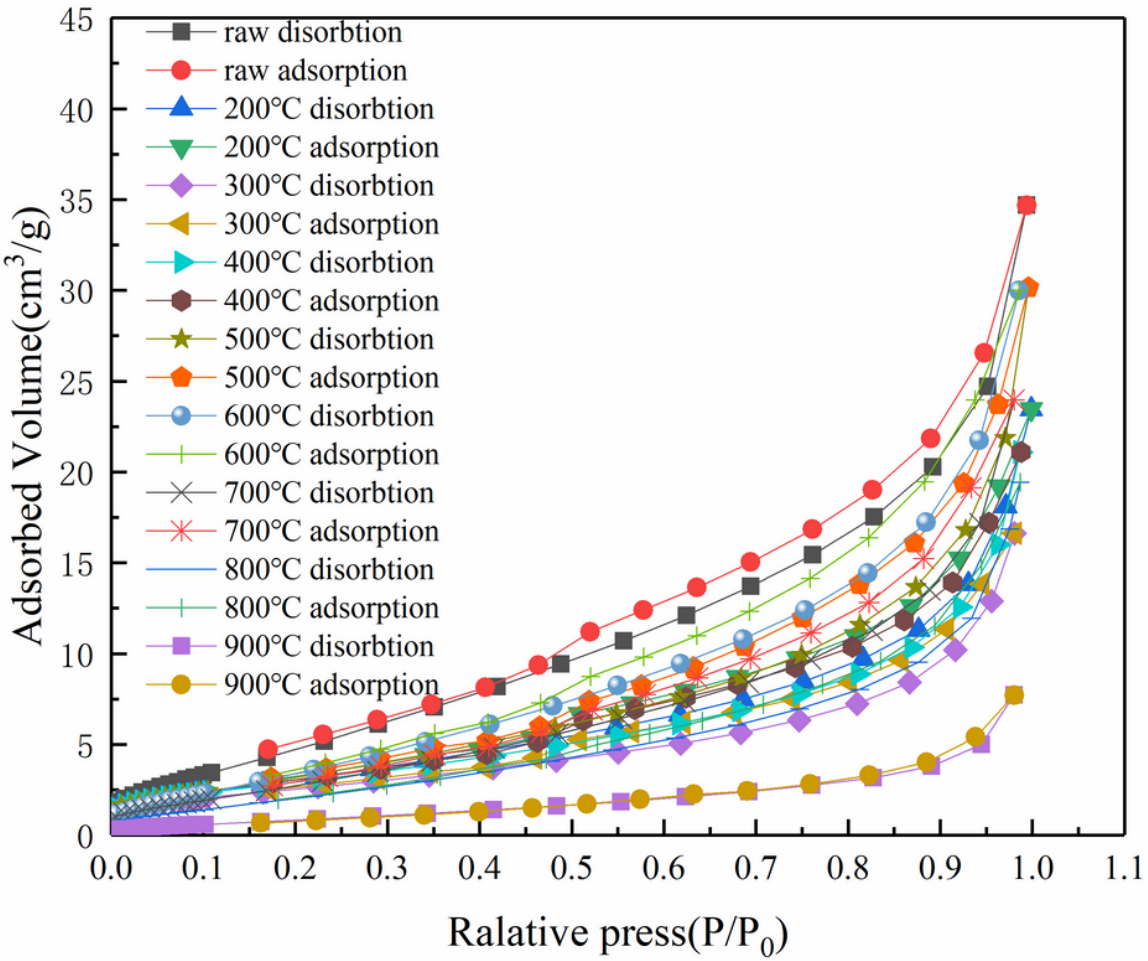

Figure 6

N_2 absorption and desorption curve of activated coal gangue at different temperatures

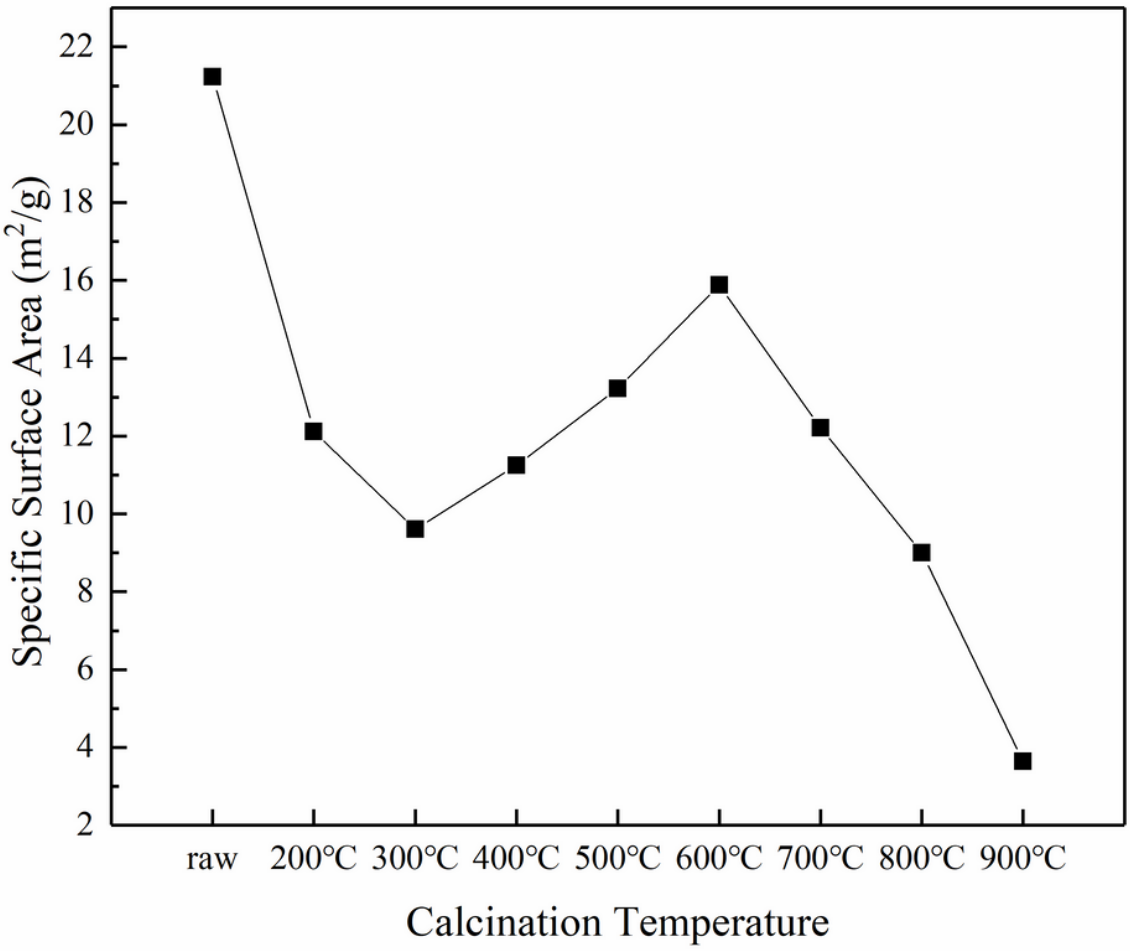

Figure 7

Specific surface change of thermally activated coal gangue

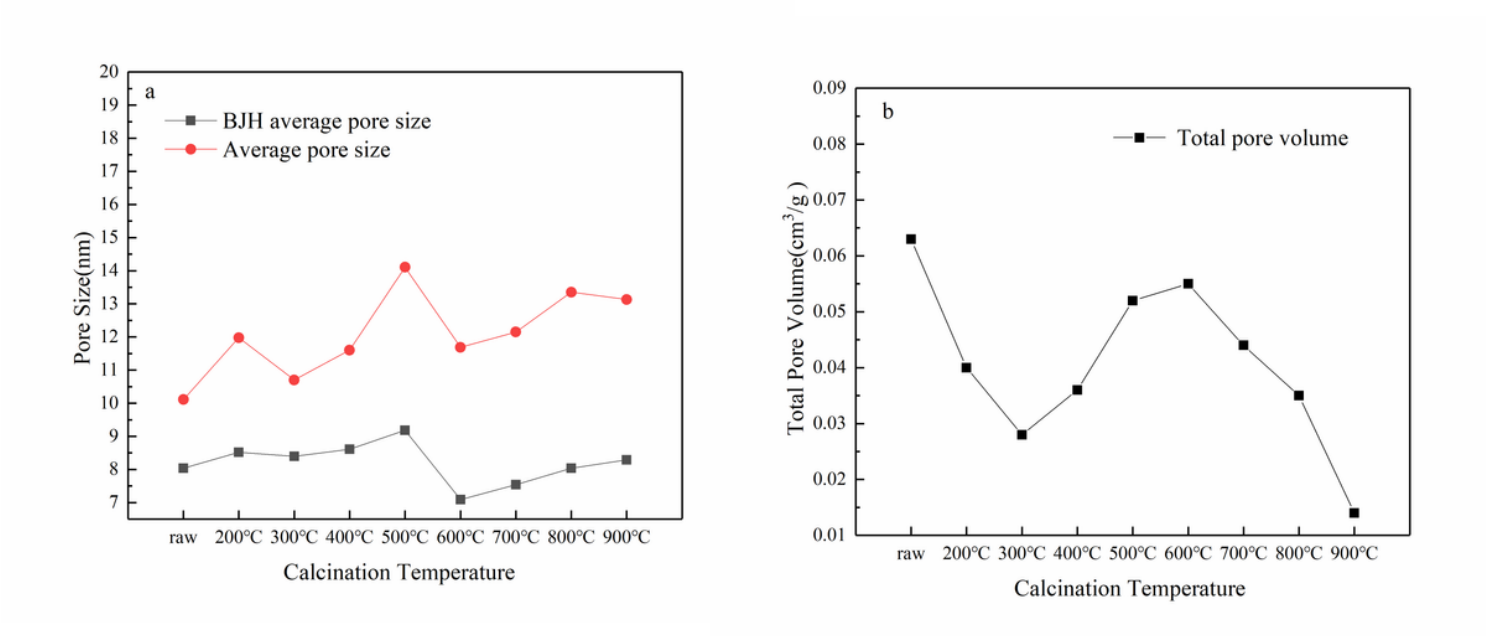

Figure 8

Succession law of pore size (a) and pore volume (b) of thermally activated coal gangue

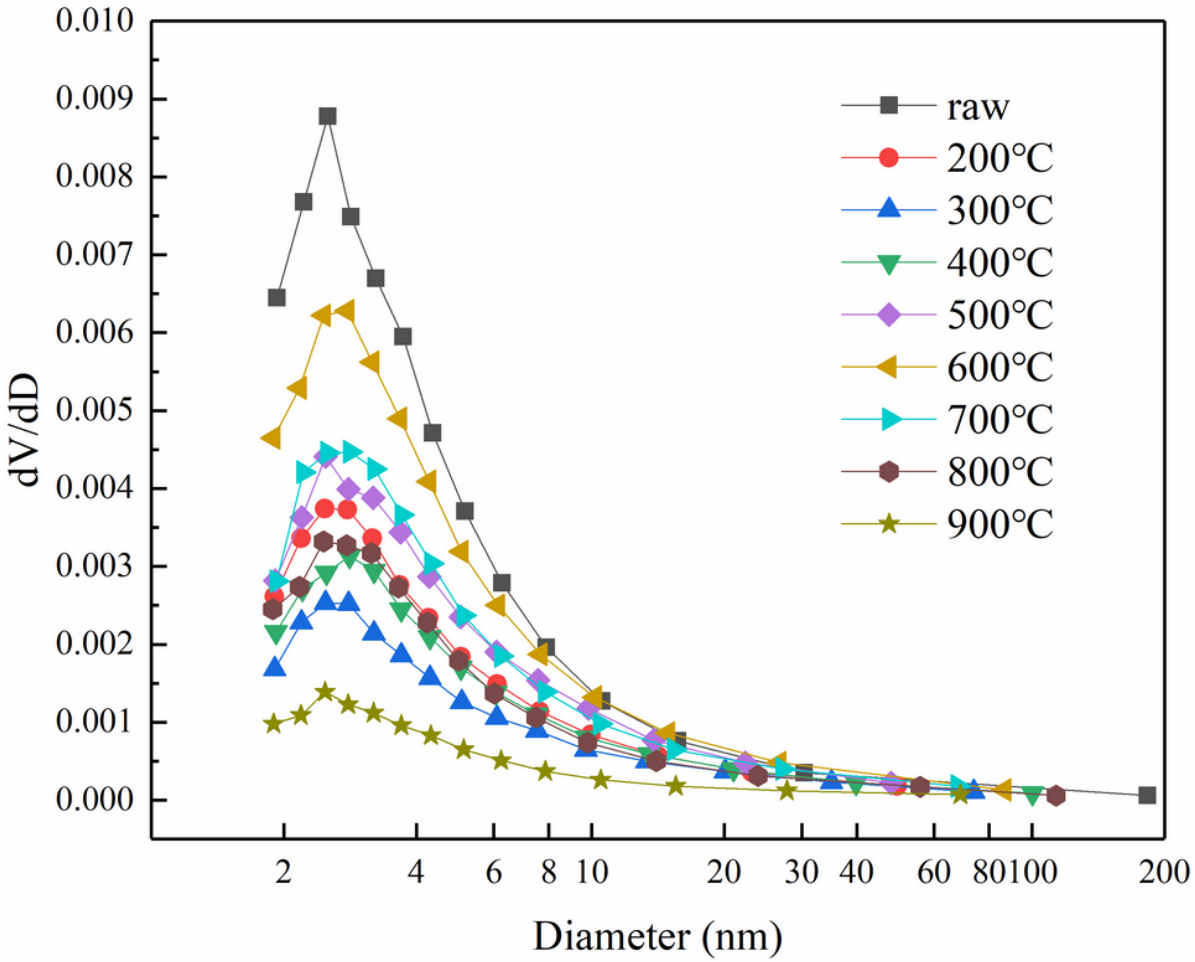

Figure 9

Succession law of pore size distribution of thermally activated coal gangue